Precoded Wake-Up Radio Signals in Multiple-Input Multiple-Output Cellular Networks

Ammar El Falou, Nour Kouzayha, Rawaa El Soufi, Charlotte Langlais

Precoded Wake-Up Radio Signals in Multiple-Input Multiple-Output Cellular Networks

Ammar El Falou[†*], Nour Kouzayha[†], Rawaa El Soufi[*], Charlotte Langlais[§]

[†] CEMSE Division, King Abdullah University of Science and Technology (KAUST), Saudi Arabia
[*] Faculty of Engineering, Lebanese University, Tripoli, Lebanon
[§] Mathematical and Electrical Department, CNRS UMR 6285 Lab-STICC, IMT Atlantique, Brest, France
Email: {ammar.falou, nour.kouzayha}@kaust.edu.sa, rawaaelsoufi@gmail.com, charlotte.langlais@imt-atlantique.fr

***Abstract*—Internet of things (IoT) presupposes a massive number of low-complexity wireless devices, placed in hardly accessible locations and often powered by batteries with limited size and capacity. To extend the lifetime of these devices, wake-up radio (WuR) techniques were proposed. In the literature, WuR solutions have been evaluated with single-antenna base stations (BSs). In this paper, we evaluate the benefits of adding multiple antennas at BSs to transmit precoded WuR signals. The considered precoded schemes provide better spatial selectivity by focusing the power of the transmitted WuR signal on the targeted devices. Monte-Carlo simulations are used to assess the performance of the system in terms of successful wake-up probability of the WuR receiver. Numerical results show that, unlike data transmission scenarios, complex precoders as multi-cell minimum mean-squared error (M-MMSE), are surpassed by the simpler maximum ratio (MR) precoder for WuR.**

***Index Terms*—Wake-up radio (WuR), precoding, multiple-input multiple-output (MIMO), cellular networks.**

I. Introduction

Energy efficiency continues to be a major challenge for the growth and large-scale deployment of battery-limited Internet of things (IoT) devices in sixth generation (6G) networks [1]. Wireless energy transfer (WET) and wake-up radio (WuR) offer effective solutions to replenish the batteries of IoT devices and activate them by wirelessly transferring sufficient amounts of radio frequency (RF) energy [2]. For energy hungry IoT devices, WuR solutions are promoted as key techniques to reduce their energy consumption and extend their batteries' lifetime [3]–[6]. An IoT device that implements WuR switches to a low-power sleep-mode whenever it is not executing a useful task. The device switches back to the active state when receiving an external on demand WuR signal with sufficient RF power to activate its main circuitry. This WuR signal is sent by a gateway/base-station (BS) with less (or no) power-constraints than IoT devices. The benefits of WuR solutions over duty-cycled medium access control (MAC) protocols for IoT systems are not only substantial energy savings but also lower latency and higher packet delivery ratio [4]. Therefore, WuR is standardized in the IEEE 802.11ba amendment [5].

The existing works on WuR consider single-antenna transmitters to transmit WuR signals [7]–[9], thus emitting power in all directions regardless of the position of the IoT devices. Therefore, the received power from single-antenna transmitters can not be always sufficient to activate the circuitry of targeted devices, which limits the range of the WuR solution and its practical deployment. Furthermore, the false wake-up probability, defined as the probability that the device wakes-up from a signal that is not intended to it, is high [10].

Multiple-input multiple-output (MIMO) techniques, such as precoding, are key technologies to increase the system capacity and improve the user experience [1], [11], [12]. In the context of data transmission, i.e., spectral efficiency (SE) enhancement, MIMO precoding techniques aim to i) focus the power transmitted by the serving BS on the targeted devices through beamforming, ii) decrease multi-user/multi-cell interference thanks to spatial selectivity.

The goal of this work is to increase the probability of successful wake-up at the IoT devices, and, in return, the range of WuR signals, thanks to the MIMO base station's beamforming ability to digitally precode WuR signals. For data transmission, different precoding schemes exist, such as multi-cell minimum mean-squared error (M-MMSE) or maximum ratio (MR) [11]. However, they differ by their computational complexity and their capability to cancel intra-cell and/or inter-cell interference. We recall that these precoders are designed for data transmission, where the interference plays a negative role on the system performance. In our context, the interference has a positive impact as it increases the overall received power at the IoT device, and hence the chance of successful wake-up [8].

Monte-Carlo simulations are used to assess the successful wake-up probability of precoded WuR signals with respect to: the type of precoder, the number of BS antennas, the wake-up threshold power and the number of devices per cell. We consider an urban macro-cell environment typical for the industry 4.0 [13], where a group of wireless IoT devices has to be waken-up by a MIMO cellular network due to an urgent or event-driven situation. The numerical results show that, unlike data transmission scenario, complex M-MMSE, designed for the maximization of the SE, doesn't provide the highest successful wake-up probability, whereas the low-complex MR precoder outperforms the other ones.

The remainder of this paper is organized as follows. Section II presents the system model and the performance metric. Section III presents the MIMO precoders. Section IV provides the numerical results. Conclusions are drawn in Section V.

Notations: $\mathbf{A}$, $\mathbf{a}$ and a denote matrix, vector and scalar respectively. $(.)^T$ and $(.)^H$ represent the transpose and the conjugate transpose respectively. $\mathcal{N}(\mu, \sigma^2)$ is the Gaussian random variable with mean μ and variance σ^2.

II. System Model

A. Network and Channel Models

We consider a downlink (DL) wireless network having L cells operating on a synchronous time division duplex (TDD) protocol. The BSs are located at the center of each cell, as depicted in Fig. 1, and have no power budget constraint. Each BS has M antennas in a uniform linear array (ULA) form ($M >> 1$) serving K single-antenna devices simultaneously ($M/K \geq 1$) [11]. Each device is equipped with a WuR receiver able to wake-up the main circuitry when it receives a sufficient amount of power, greater than a threshold.

1) Transmitter side: The BS in the l-th cell, denoted by BS l, sends the DL signal

$$\mathbf{x}_l = \sum_{i=1}^{K} \mathbf{w}_{li}\zeta_{li}, \tag{1}$$

where ζ_{li} is the signal intended for device i in cell l. This signal is multiplied by a precoding vector $\mathbf{w}_{li} \in \mathbb{C}^M$ determining the directivity of the transmitted signal. The precoding vector $\mathbf{w}_{li}$ is normalized, i.e., $\mathbb{E}\{\|\mathbf{w}_{li}\|^2\} = 1$. $\mathbb{E}\{\|\mathbf{w}_{li}\zeta_{li}\|^2\} = \rho_{li}$ is then the transmit power assigned to device i.

2) Receiver side: At device k in cell j, the received signal y_{jk} is given by (see Fig. 1)

$$\begin{aligned} y_{jk} &= \sum_{l=1}^{L} \left(\mathbf{h}_{jk}^{l}\right)^H \mathbf{x}_l + \eta_{jk} \\ &= \sum_{l=1}^{L}\sum_{i=1}^{K} \left(\mathbf{h}_{jk}^{l}\right)^H \mathbf{w}_{li}\zeta_{li} + \eta_{jk} \\ &= \underbrace{\left(\mathbf{h}_{jk}^{j}\right)^H \mathbf{w}_{jk}\zeta_{jk}}_{\text{Intended signal } (i=k,\, l=j)} + \underbrace{\sum_{i=1, i\neq k}^{K} \left(\mathbf{h}_{jk}^{j}\right)^H \mathbf{w}_{ji}\zeta_{ji}}_{\text{Intra-cell interference } (i\neq k,\, l=j)} \\ &+ \underbrace{\sum_{l=1, l\neq j}^{L}\sum_{i=1}^{K} \left(\mathbf{h}_{jk}^{l}\right)^H \mathbf{w}_{li}\zeta_{li}}_{\text{Inter-cell interference } (l\neq j)} + \underbrace{\eta_{jk}}_{\text{Noise}}, \end{aligned} \tag{2}$$

where $\eta_{jk} \sim \mathcal{N}_{\mathbb{C}}(0, \sigma^2)$ is the independent additive complex noise with variance σ^2. $\mathbf{h}_{jk}^{l} \in \mathbb{C}^M$ represents the channel coefficient between device k in cell j and the BS l. The channel state information (CSI) is assumed to be known at the BSs through estimation. The channel coefficients h_{jk}^{l} are constant within a coherence block.

In this work, we consider a correlated Rayleigh fading channel, i.e., $h_{jk}^{l} \sim N_{\mathbb{C}}(\mathbf{0}_M, \mathbf{R}_{jk}^{l})$. The spatial correlation matrices $\mathbf{R}_{jk}^{l}$ are generated using the Gaussian local scattering model with angular standard deviation (ASD) of 10° typical for urban macro-cell networks. $\mathbf{R}_{jk}^{l}$ describes the macroscopic propagation effects, including the path-loss, the shadowing, the antenna gains and radiation patterns at the transmitters and receivers (see [11] and references therein).

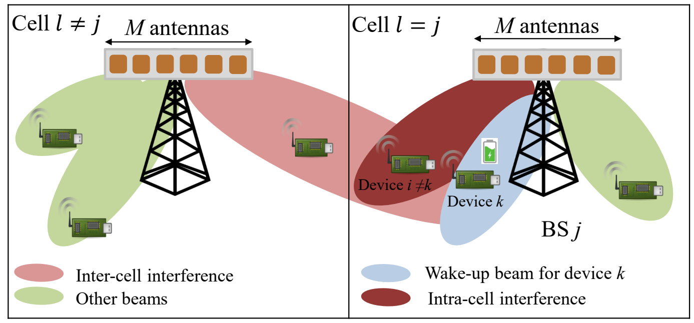

Fig. 1. System model.

B. Performance Metric

In this paper, we focus on the computation of the successful wake-up probability of the WuR receiver, when the transmitted WuR signals are precoded. The successful wake-up probability of device k in cell j, denoted as Pr_{jk}, is defined as the probability that the received power P_{jk} is greater than a threshold P_{Th} and is given by

$$\text{Pr}_{jk} = \mathbb{P}[P_{jk} \geq P_{\text{Th}}], \tag{3}$$

where P_{Th} is the power threshold required to achieve a successful wake-up and defines the sensitivity of the added wake-up module to the IoT device. Achieving higher sensitivities is a design target to increase the wake-up range [14].

The received power P_{jk} of device k in cell j can be computed from the expression of y_{jk} in (2) as the power of all received signals from all BSs, i.e., the power of the signal

$$\begin{aligned} \sum_{l=1}^{L}\sum_{i=1}^{K} \left(\mathbf{h}_{jk}^{l}\right)^H \mathbf{w}_{li}\zeta_{li} &= \underbrace{\left(\mathbf{h}_{jk}^{j}\right)^H \mathbf{w}_{jk}\zeta_{jk}}_{\text{Intended signal } (i=k,\, l=j)} + \\ \underbrace{\sum_{i=1, i\neq k}^{K} \left(\mathbf{h}_{jk}^{j}\right)^H \mathbf{w}_{ji}\zeta_{ji}}_{\text{Intra-cell interference } (i\neq k,\, l=j)} &+ \underbrace{\sum_{l=1, l\neq j}^{L}\sum_{i=1}^{K} \left(\mathbf{h}_{jk}^{l}\right)^H \mathbf{w}_{li}\zeta_{li}}_{\text{Inter-cell interference } (l\neq j)}. \end{aligned} \tag{4}$$

It is clear from (4) that, contrary to the case of data transmission, the interference here has a positive impact on the successful wake-up as it increases the received power by the device. The value of the received power highly depends on the choice of MIMO precoders, presented in the following section.

III. MIMO Precoders

For notational convenience, we define $\hat{\mathbf{H}}_{j}^{l}$ as the $M \times K$ matrix with all channel estimates from the M antennas of BS l, to K devices in cell j

$$\hat{\mathbf{H}}_{j}^{l} = [\hat{\mathbf{h}}_{j1}^{l} \ldots \hat{\mathbf{h}}_{jK}^{l}]. \tag{8}$$

M-MMSE, S-MMSE, RZF, ZF and MR precoders are considered. Their DL precoding vectors are given by

$$\mathbf{w}_{lk} = \frac{\mathbf{v}_{lk}}{\|\mathbf{v}_{lk}\|}, \tag{9}$$

where

$$[\mathbf{v}_{l1} \dots \mathbf{v}_{lK}] = \begin{cases} \mathbf{V}_l^{\text{M-MMSE}} & \text{for M-MMSE} \\ \mathbf{V}_l^{\text{S-MMSE}} & \text{for S-MMSE} \\ \mathbf{V}_l^{\text{RZF}} & \text{for RZF} \\ \mathbf{V}_l^{\text{ZF}} & \text{for ZF} \\ \mathbf{V}_l^{\text{MR}} & \text{for MR} \end{cases} \tag{10}$$

The characteristics of the aforementioned precoders and the combining matrices of MR and ZF are defined in the sequel. The equations of the combining matrices for RZF, S-MMSE and M-MMSE can be found in [11]. We recall that these precoders are designed for data transmission where decreasing the interference is their main objective.

1) Maximum Ratio: The MR precoding aims to focus the DL signal at the targeted device in order to guarantee the maximum array gain. The corresponding matrix is given as

$$\mathbf{V}_l^{\text{MR}} = \hat{\mathbf{H}}_l^l. \tag{11}$$

We highlight that the MR precoding does not need matrix inversion. The remaining precoders are more complex as they require matrix inversion with different sizes.

2) Zero Forcing: ZF precoder aims to cancel all the interference from intra-cell devices while keeping the desired signals non-zero. The ZF combining matrix is given as follows

$$\mathbf{V}_l^{\text{ZF}} = \hat{\mathbf{H}}_l^l \left((\hat{\mathbf{H}}_l^l)^H \hat{\mathbf{H}}_l^l \right)^{-1}. \tag{12}$$

ZF successfully eliminates the intra-cell interference for high signal-to-noise ratio (SNR) devices. It is clear that the matrix inversion is possible only if the $K \times K$ matrix $(\hat{\mathbf{H}}_l^l)^H \hat{\mathbf{H}}_l^l$ has full rank, which is usually the case when $M >> K$, but not necessarily when $M \approx K$.

3) Regularized ZF: RZF is a regularized form of ZF. The regularization refers to the fact that the inverted $K \times K$ matrix is regularized by a diagonal matrix depending on the noise variance. This regularization enhances the numerical stability of the matrix inversion. In terms of precoding, it provides a weighting between a maximization of the intended signals (for large regularization terms) and an interference suppression (for small regularization terms).

4) Multiple and Single MMSE: M-MMSE aims to maximize the instantaneous signal-to-interference-plus-noise ratio (SINR) and minimize the mean-squared error (MSE) between the desired and received signals in the detection of data. M-MMSE precoding is optimal for DL SE. However, in addition to the inversion of an $M \times M$ matrix, M-MMSE requires a full coordination between cells and a knowledge of all channel coefficients between all cells and devices in the network.

On the other hand, S-MMSE requires only the channel coefficients between the BS and its served devices. S-MMSE is identical to M-MMSE for a single-cell system. However, it is not able to remove interference from signals sent to devices in other cells. For data transmission, this becomes a problem when edge devices in close cells produce strong interference on intra-cell devices. The advantage of M-MMSE over S-MMSE is apparent when the level of inter-cell interference in the system is high.

TABLE I
SYSTEM PARAMETERS

Parameter	Value
Layout	Square pattern
Number of cells	$L = 16$
Cell size	0.75 km $\times$ 0.75 km
Number of antennas per BS	$M \in [10, 100]$
Number of devices per cell	$K \in [1, 10]$
Bandwidth	$B = 20$ MHz
Carrier frequency	$f_c = 2$ GHz
DL transmit power per device	10 mW
Samples per coherence block	$\tau_c = 2000$

IV. NUMERICAL RESULTS

In this section, we assess the successful wake-up probability of IoT devices when WuR signals are precoded at BSs. We recall that the main objective of this work is not to assess spectral efficiency of data transmission but the ability of the precoded WuR signals to increase the WuR range thanks to a better successful wake-up probability. However, the SE curves are still provided in the sequel for illustration.

A. System Description

The network is composed of $L = 16$ cells where each cell has an area of 0.75×0.75 km^2 and the total network area is 9 km^2. This can represent the size of a large industrial zone or a small city. Table I summarizes the system parameters. K devices per cell and M antennas per BS are considered. The same DL transmit power of 10 mW is allocated per device. The propagation parameters are inspired from the non-line-of-sight macro-cell 3GPP model [11]. The same frequency is used in all cells. Each coherence block is composed of $\tau_c = 2000$ samples. An MMSE channel estimation is performed.

B. Spectral Efficiency

For illustration, we start by plotting the well-known average DL sum SE of the presented precoders schemes in Fig. 2 with respect to the number of BS antennas M. As in [11], Fig. 2 shows that M-MMSE provides the highest sum SE for any M. S-MMSE and RZF give almost the same SE. The advantage of M-MMSE over S-MMSE and RZF is not apparent here as the transmit power is not high, thus the level of inter-cell interference in the system is low. ZF works well when the number of antennas M is much greater than the number of devices K, but has issues when M is close to K. Finally, the lowest SE is obtained using MR. Indeed, for a large M, MR reaches only 76% of the sum SE achieved by other precoders.

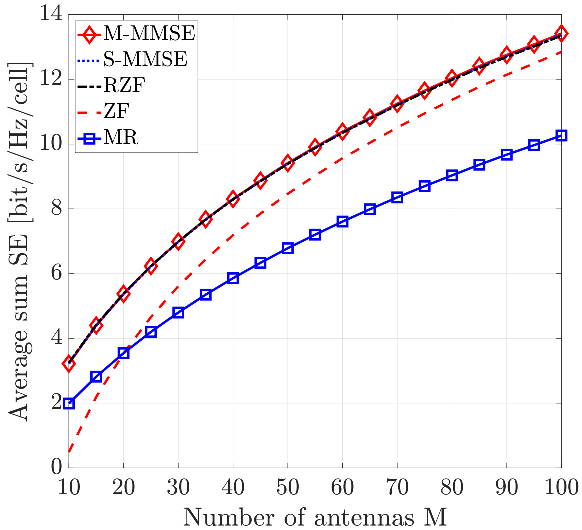

Fig. 2. Average DL sum SE with respect to M for different precoding techniques. The number of devices per cell $K = 10$.

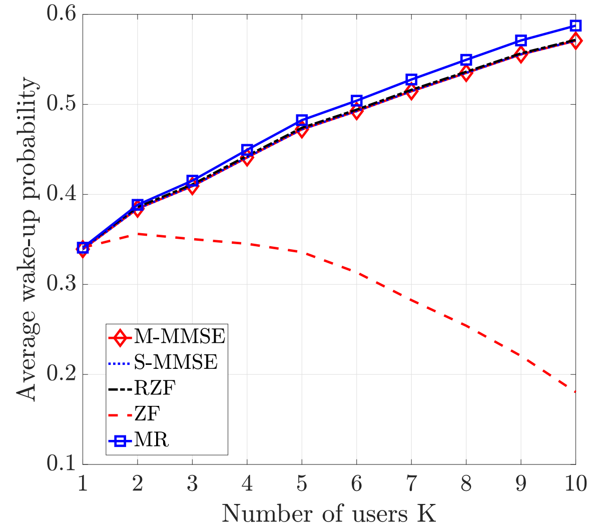

Fig. 4. Wake-up probability with respect to K when $M = 10$ and $P_{\text{Th}} = -10$ dBm.

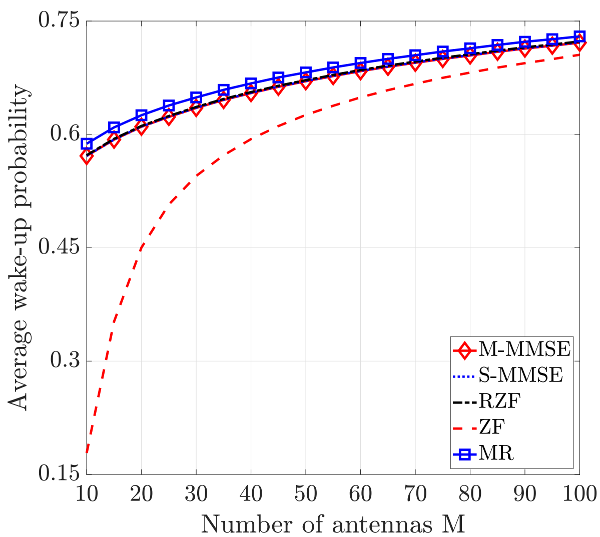

Fig. 3. Wake-up probability with respect to M when $K = 10$ and $P_{\text{Th}} = -10$ dBm.

C. *Successful Average Wake-up Probability per Device*

In this section, we plot the empirical average wake-up probability of the IoT devices when WuR signals are precoded with respect to several system parameters as: the type of MIMO precoders, the number of BS antennas M, the number of devices per cell K and the wake-up threshold P_{Th}. We highlight here that the RF wake-up signals are sent to all $K \times L$ devices, typical of IoT systems, and that the successful wake-up probability is averaged over them.

Fig. 3 plots the average wake-up probability per device with respect to the number of BS antennas M for $K = 10$ devices per cell and a wake-up threshold of $P_{\text{Th}} = -10$ dBm. It shows that the MR precoder has the highest wake-up probability, followed by M-MMSE, S-MMSE and RZF. ZF provides the lowest wake-up probability especially when M is close K. Indeed, when the number of devices is close to the number of antennas, ZF fails to focus the power at the IoT devices, thus reducing their received power, and decreasing their successful wake-up probability.

The successful average wake-up probability per device increases for all precoders with the increase of M, thanks to the beamforming gain. Indeed, by using MR, the wake-up probability increases from 0.58 when $M = 10$ to 0.72 when $M = 100$ (massive MIMO BSs). For single antenna BSs ($M = 1$), the successful wake-up probability is only 0.49.

The advantage of MR over the remaining schemes can be explained by the fact that performant precoders are designed to decrease the intra-cell interference (ZF, RZF and S-MMSE) and intra/inter-cell interference (M-MMSE). On the other side, MR focuses the power in the direction of devices without taking care of interference. When the devices are close to each other, the produced interference plays a positive role for wake-up by increasing the received power at the IoT devices [8].

Fig. 4 plots the average wake-up probability per device with respect to the number of devices per cell K, with a number of BS antennas $M = 10$. It clearly shows that the wake-up probability increases with the number of devices per cell using all the precoding schemes except ZF. Moreover, MR provides the highest value. M-MMSE, S-MMSE and RZF are very similar. Indeed, the wake-up probability for MR, M-MMSE, S-MMSE and RZF increases as the WuR system can benefit from the intra-cell interference. ZF is almost stable at the beginning as it is able to cancel the intra-cell interference when $M >> K$. However, when the number of devices becomes close to the number of antennas, i.e., when $M \approx K$, it fails to focus the power at the devices and thus its wake-up probability rapidly decreases.

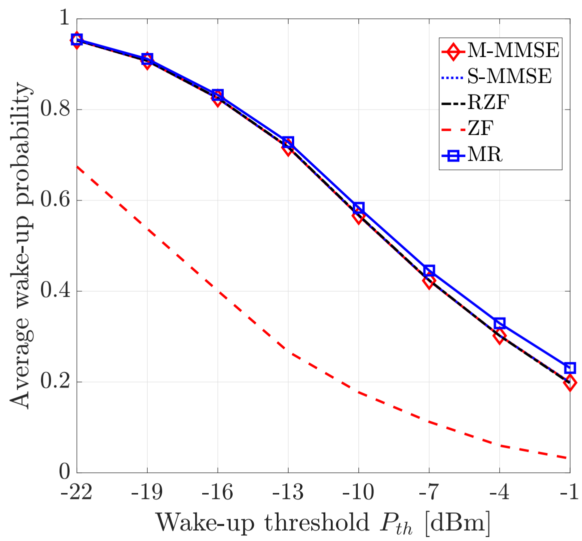

Fig. 5. Wake-up probability with respect to P_{Th} when $K = M = 10$.

Fig. 5 plots the wake-up probability with respect to the wake-up threshold P_{Th}. The figure shows that the wake-up probability is close to one for all precoders except ZF for a low value of P_{Th}. This value decreases when P_{Th} increases, with a superiority for MR over the remaining precoders. Again as $M = K$, ZF is not able to focus the power to the devices and it provides a low wake-up probability.

V. Conclusion

In this work, we proposed the use of MIMO precoded WuR signals, that greatly improve the successful wake-up probability by focusing the transmitted power on the IoT devices. Moreover, simulation results have shown that well-known precoders, designed for data transmission, do not provide the highest wake-up probability. Thus, the simple MR precoder outperforms complex precoders, such as M-MMSE or RZF. Indeed, interference plays a positive role for WuR whereas conventional MIMO precoders are designed to reduce this interference. In practical systems, it is clear that different precoders have to be employed either for WuR or data transmission.

As future works, we plan to assess the spatial selectivity of these precoders, i.e., their ability to successfully wake-up a desired device without altering the state of nearby non-desired devices. A selective wake-up is important to decrease the false wake-up probability without the need to incorporate additional hardware as address decoder, as the one proposed in [15], [16]. One important perspective of this work is the study of channel estimation for WuR. Indeed, a periodic channel estimation is not an option as it eliminates the advantage of on-demand WuR in reducing the unnecessary energy consumption of the device. Considering a synchronous TDD duplex system, the channel estimation has to be done in the uplink when the devices transmit their data to the BSs. The accuracy of this estimation will highly depend on the stationarity of the environment. One possible alternative solution is the use of MIMO precoders requiring only partial CSI as the angle of departure (AoD) of line of sight (LoS) paths [17], [18]. The estimation of the AoD requires low-complex and low-overhead algorithms with respect to full CSI case.

References

[1] S. Dang, O. Amin, B. Shihada, and M.-S. Alouini, "What should 6G be?" *Nature Electronics*, vol. 3, no. 1, pp. 20–29, 2020.

[2] D. Niyato, D. I. Kim, M. Maso, and Z. Han, "Wireless powered communication networks: Research directions and technological approaches," *IEEE Wireless Communications*, vol. 24, no. 6, pp. 88–97, 2017.

[3] R. Piyare, A. L. Murphy, C. Kiraly, P. Tosato, and D. Brunelli, "Ultra low power wake-up radios: A hardware and networking survey," *IEEE Commun. Surveys & Tuts.*, vol. 19, no. 4, pp. 2117–2157, 2017.

[4] J. Oller, I. Demirkol, J. Casademont, J. Paradells, G. U. Gamm, and L. Reindl, "Has time come to switch from duty-cycled MAC protocols to wake-up radio for wireless sensor networks?" *IEEE/ACM Trans. on Netw.*, vol. 24, no. 2, pp. 674–687, 2015.

[5] IEEE 802.11ba-2021, "IEEE standard for information technology–telecommunications and information exchange between systems–local and metropolitan area networks-specific requirements – Part 11: Wireless lan medium access control (MAC) and physical layer (PHY) specifications – Amendment 3: Wake-up radio operation," *IEEE Std*, 2021.

[6] D. E. Ruiz-Guirola, C. A. Rodríguez-López, S. Montejo-Sánchez, R. D. Souza, O. L. López, and H. Alves, "Energy-efficient wake-up signalling for machine-type devices based on traffic-aware long-short term memory prediction," *IEEE Internet of Things Journal*, 2022.

[7] N. Kouzayha, Z. Dawy, J. G. Andrews, and H. ElSawy, "Joint downlink/uplink RF wake-up solution for IoT over cellular networks," *IEEE Trans. Wireless Commun.*, vol. 17, no. 3, pp. 1574–1588, 2017.

[8] S. Saab, N. Kouzayha, J. Costantine, and Z. Dawy, "Positive impact of interference on RF energy harvesting for IoT devices," in *Proc. IEEE Int. Symp. on Personal, Indoor and Mobile Radio Commun. (PIMRC)*, 2018, pp. 312–317.

[9] H. Bello, Z. Xiaoping, R. Nordin, and J. Xin, "Advances and opportunities in passive wake-up radios with wireless energy harvesting for the internet of things applications," *Sensors*, vol. 19, no. 14, 2019.

[10] A. A. Benbuk, N. Kouzayha, J. Costantine, and Z. Dawy, "Tunable, asynchronous, and nanopower baseband receiver for charging and wake-up of IoT devices," *IEEE Internet of Things Journal*, 2021.

[11] E. Björnson, J. Hoydis, and L. Sanguinetti, "Massive MIMO networks: Spectral, energy, and hardware efficiency," *Foundations and Trends in Signal Processing*, vol. 11, no. 3-4, pp. 154–655, 2017.

[12] I. Khaled, C. Langlais, A. El Falou, B. A. Elhassan, and M. Jezequel, "Multi-user angle-domain MIMO-NOMA system for mmWave communications," *IEEE Access*, vol. 9, pp. 129 443–129 459, 2021.

[13] G. Aceto, V. Persico, and A. Pescapé, "A survey on information and communication technologies for industry 4.0: State-of-the-art, taxonomies, perspectives, and challenges," *IEEE Commun. Surveys & Tuts.*, vol. 21, no. 4, pp. 3467–3501, 2019.

[14] M. Magno, V. Jelicic, B. Srbinovski, V. Bilas, E. Popovici, and L. Benini, "Design, implementation, and performance evaluation of a flexible low-latency nanowatt wake-up radio receiver," *IEEE Trans. on Ind. Informat.*, vol. 12, no. 2, pp. 633–644, 2016.

[15] P. Le-Huy and S. Roy, "Low-power wake-up radio for wireless sensor networks," *Mobile Networks and Applications*, vol. 15, no. 2, pp. 226–236, 2010.

[16] H. Khodr, N. Kouzayha, M. Abdallah, J. Costantine, and Z. Dawy, "Energy efficient IoT sensor with RF wake-up and addressing capability," *IEEE Sensors Lett.*, vol. 1, no. 6, pp. 1–4, 2017.

[17] I. Khaled, A. El Falou, C. Langlais, B. ELHassan, and M. Jezequel, "Multi-user digital beamforming based on path angle information for mm-Wave MIMO systems," in *Proc. International ITG Workshop on Smart Antennas (WSA)*, 2020.

[18] I. Khaled, C. Langlais, A. El Falou, M. Jezequel, and B. Elhasssan, "Joint single-and multi-beam angle-domain noma for hybrid mmwave mimo systems," in *Proc. International ITG Workshop on Smart Antennas (WSA)*, 2021.